

Advanced luminescence based effective series resistance imaging of silicon solar cells

H. Kampwerth,^{1,a)} T. Trupke,² J. W. Weber,¹ and Y. Augarten¹

¹Centre of Excellence for Advanced Silicon Photovoltaics and Photonics, University of New South Wales, Sydney 2052, Australia

²BT Imaging Pty. Ltd., NSW, Sydney 2000, Australia

(Received 30 July 2008; accepted 26 August 2008; published online 18 November 2008)

A technique for fast and spatially resolved measurement of the effective series resistance of silicon solar cells from luminescence images is introduced. Without compromising the speed of existing luminescence based series resistance imaging methods, this method offers significant advantages in that it is more robust against variations in local diode characteristics. Lateral variations in the series resistance of an industrial screen printed multicrystalline silicon solar cell obtained from this method show excellent correlation with a Corescan measurement and are also shown to be unaffected by lateral variations in the diode properties. © 2008 American Institute of Physics.

[DOI: 10.1063/1.2982588]

A critical electrical parameter of solar cells that can vary noticeably across the cell area is the series resistance R_S . Existing experimental techniques to measure the spatial variation in the series resistance include scanning techniques such as Corescan¹ and Cello² as well as imaging techniques such as infrared lock-in thermography.^{3,4} Typical data acquisition times of these methods are of the order of several minutes to hours per solar cell. Using luminescence imaging as a significantly faster alternative for spatially resolved measurements of the series resistance was proposed and demonstrated in Ref. 5. Several quantitative luminescence based R_S -imaging methods have been suggested since then.^{6–8} One challenge with these methods is that the analysis of luminescence images in terms of absolute values for the series resistance can be strongly affected by the local diode parameters, which are generally not known, especially in multicrystalline (mc) cells that can lead to inaccuracies due to large variations in diode parameters across the cell.

In our experimental setup a 815 nm/50 W laser illuminates the cell area homogeneously with up to 1 sun equivalent photogeneration rate. Luminescence images are taken at various illumination intensities and terminal voltages using a cooled charge coupled device camera.

In our theoretical model the solar cell is described as a two dimensional network of parallel individual nodes. Each node i contains a current source J_{light} , an unknown dark current density $J_{\text{dark},i}(U_i)$, and a series resistance $R_{S,i}$ (see Fig. 1). The characteristics of $J_{\text{dark},i}(U_i)$ can be modeled by the commonly used two-diode model, which includes a shunt resistance parallel to the diodes.

In this model $R_{S,i}$ is the effective series resistance of node i at a given operating point of the cell, which is the sum of all series and transport resistances in the current path from one terminal through that node to the other terminal. It also includes light generated effects of current generation and recombination of other nodes in the current path.

Similar to the method described by Trupke *et al.*,⁶ the method to be discussed here is based on the analysis of two

luminescence intensities for each pixel taken under different operating conditions. Basic analysis shows that the series resistance in units of $\Omega \text{ cm}^2$ is given as

$$R_{S,i} = \frac{\Delta U_{R_{S,i}}}{\Delta J_{R_{S,i}}} = \frac{\Delta U_i - \Delta U_{\text{term}}}{\Delta J_{\text{light}} - \Delta J_{\text{dark},i}}, \quad (1)$$

where $\Delta U_{R_{S,i}}$ is the difference in voltages across the series resistance between the two operating points and $\Delta J_{R_{S,i}}$ is the difference in current densities. These can be expressed by the differences in local diode voltage ΔU_i , the difference in terminal voltage ΔU_{term} , the difference in light generated current density ΔJ_{light} , and the difference in dark current density $\Delta J_{\text{dark},i}$. These quantities are shown in Fig. 2, which schematically depicts the situation where a solar cell is operated at two different operating points corresponding to the same diode voltage U_i .

In previous luminescence based R_S -methods, inaccuracies are associated with the determination or approximation of ΔU_i and $\Delta J_{\text{dark},i}$. The key feature of the method presented here is to remove the need for conversion of luminescence intensities into absolute voltages and the need to make assumptions about $J_{\text{dark}}(U_i)$. This is achieved by choosing two different solar cell operating points that result in the same luminescence intensity $I_{\text{camera},i}$.

As will be discussed below, measuring identical offset corrected luminescence signals at two different operating conditions is equivalent to identical diode voltages U_i . As a result $\Delta U_i = 0$ in Eq. (1). Identical diode voltages correspond

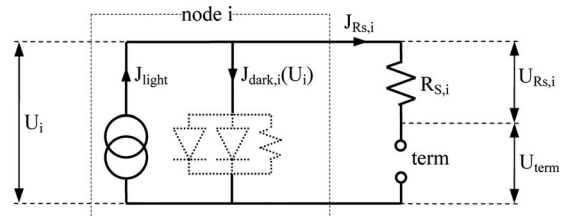


FIG. 1. Equivalent circuit of one node at position i , which corresponds to image pixel i , containing a current source J_{light} , the dark current $J_{\text{dark},i}$, and a series resistance $R_{S,i}$.

^{a)}Tel.: +61-2-9385-6057. FAX: +61-2-9385-5104. Electronic mail: h.kampwerth@student.unsw.edu.au.

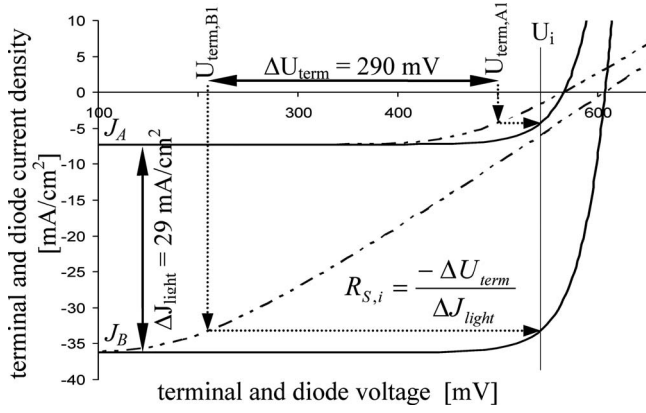


FIG. 2. I - V curves of one node i at two illumination intensities with $J_{\text{light},A1}=7 \text{ mA/cm}^2$ and $J_{\text{light},B1}=36 \text{ mA/cm}^2$. Solid curves are the I - V characteristics without series resistance (i.e., current density as a function of the diode voltage). Broken curves include the effect of series resistance of $10 \text{ } \Omega \text{ cm}^2$. The solid vertical line represents the diode voltage U_i , corresponding to terminal voltages $U_{\text{term},A1}$ and $U_{\text{term},B1}$.

to identical dark current densities, which result in $\Delta J_{\text{dark},i}=0$. Under these assumptions Eq. (1) simplifies to

$$R_{S,i} = \left. \frac{-\Delta U_{\text{term}}}{\Delta J_{\text{light}}} \right|_{\Delta U_i=0}, \quad (2)$$

where ΔU_{term} is easily measured between the terminals and J_{light} is the difference in short circuit current densities. The latter can also be measured at the terminals under the assumption that the short circuit current density is approximately constant across the cell.

The above correlation between luminescence signal and local diode voltage can be made since the luminescence signal is an exponential function of the local diode voltage U_i ,^{9,10}

$$I_{\text{camera},i} = C_i \exp\left(\frac{eU_i}{kT}\right) + C_{\text{offset},i}, \quad (3)$$

where e is the electron charge, k the Boltzmann constant, and T the junction temperature. C_i is a voltage dependent calibration constant,¹¹ which accounts for locally varying optical properties and variations in the luminescence signal of the cell due to variations in the local diffusion length of minority carriers.¹¹ A junction voltage independent offset of the luminescence signal $C_{\text{offset},i}$ is caused by radiative recombination of diffusion-limited carriers.⁶ This constant can be measured experimentally for a given illumination intensity and for each pixel by taking a luminescence image at short circuit conditions.⁶ Our experiments show that in cases of very high local series resistance, it is necessary to even go into reverse bias to ensure that the exponential term in Eq. (3) is negligible.

In practice all luminescence images have to be corrected to eliminate the offset $C_{\text{offset},i}$, as discussed above. All images referred to below are offset corrected.

For the proposed measurement procedure, a first luminescence measurement A is carried out at an incident light intensity $I_{\text{illum},A}$ and with terminal voltage $U_{\text{term},A}$, followed by a second luminescence measurement B at $I_{\text{illum},B}$ and terminal voltage $U_{\text{term},B}$. For identical luminescence signals in

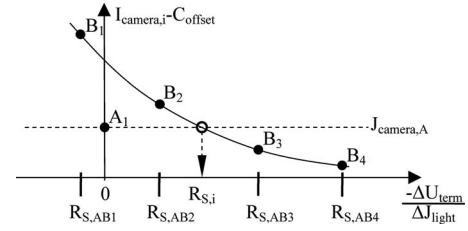


FIG. 3. Offset-corrected luminescence signal as a function of changed operation condition between image A and image B ($-\Delta U_{\text{term}}/\Delta J_{\text{light}}$) or values of $R_{S,i}$ according to Eq. (3). The luminescence intensity in measurement B, which corresponds to measurement A, determines the correct value for the series resistance.

the two measurements, the series resistance is then calculated according to Eq. (2), with ΔJ_{light} given by the difference in short circuit currents.

The condition of identical luminescence intensity will not be fulfilled for most pixels in two luminescence images A and B. However, a broad range of series resistance values can be accurately obtained with a small number of images B, measured at constant illumination $I_{\text{illum},B}$ and variable terminal voltages $U_{\text{term},B}$. Each different terminal voltage $U_{\text{term},B}$ corresponds to a possible series resistance value according to Eq. (2). The correct series resistance can be determined via interpolation as shown in Fig. 3, a procedure that can be applied to each pixel. This same method is applicable for a series of images B during which either the illumination intensity or both the illumination intensity and the terminal voltage are varied.

This method is demonstrated on an industrial mc silicon solar cell. In total six images were taken at various terminal voltages and with two different light intensities. One of the images was taken at open circuit condition and is shown in Fig. 4 (left). Variations in the local diode voltage and in the local diffusion length¹² result in variations in the luminescence intensity.

The right hand side of Fig. 4 shows the effective R_S -image of the same part of the solar cell (color scale gives the series resistance in $\Omega \text{ cm}^2$) measured using the method described above and the following measurement conditions:

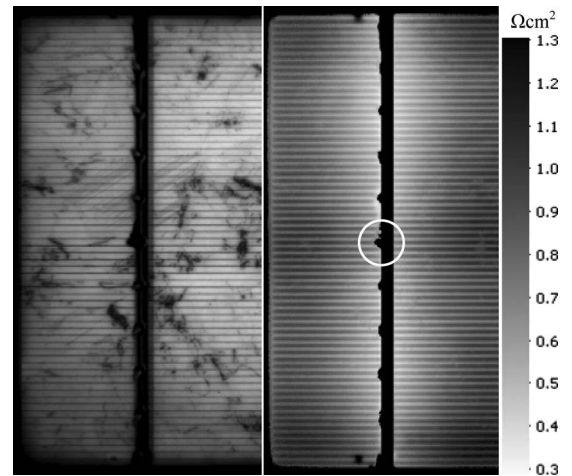


FIG. 4. Left: PL image of one-half of a mc-Si solar cell at V_{OC} condition. Variations in lifetime and diode characteristics are visible. Bright regions represent high voltage/accordingly lifetime. Right: R_S -image created by proposed method of the same part of solar cell. The R_S values are nearly free of effects of varying diode characteristics and lifetimes.

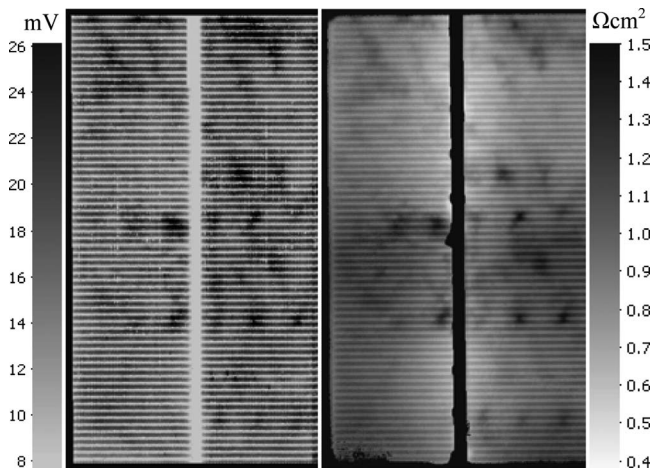


FIG. 5. Left: Corescan image showing the voltage drop toward the terminal. Right: R_S -image of the same part of solar cell. Identical areas of high series resistance are observed in both images.

$U_{\text{term,A}}=650$ mV, $J_{\text{light,A}}=0$ mA/cm², $U_{\text{term,B}}=600-650$ mV, and $J_{\text{light,B}}=35$ mA/cm². The R_S -image is unaffected by the fluctuations of local diode characteristics seen on the left hand side of Fig. 4.

The cell was contacted along the busbars in a four point probe arrangement with arrays of spring loaded pins. The center pin on the front busbar (circle in Fig. 4) measures the voltage and is not used for current extraction or injection. The R_S -image reveals that the series resistance is higher in the vicinity of the voltage pin, showing that the measured series resistance is not only a feature of the cell but also depends on how the cell is contacted. Other features in the R_S -image in Fig. 4 are associated with the current transport through the metal fingers and the emitter.

Figure 5 shows a series resistance image (in Ω cm²) of a different mc-Si solar cell, obtained with $U_{\text{term,A}}=570$ mV, $J_{\text{light,A}}=0$ mA/cm², $U_{\text{term,B}}=570-520$ mV, and $J_{\text{light,B}}=35$ mA/cm². The voltage drop between the front busbar and the emitter (in mV) obtained from Corescan¹ is shown on the left. The latter was performed with a line spacing of 0.5 mm and with illumination equivalent to 30 mA/cm² short circuit current density.

The same areas of enhanced series resistance are qualitatively observed with both methods, indicating that these features are caused by enhanced contact resistance at the front. A quantitative correlation between the spatially resolved R_S values from photoluminescence (PL)-imaging and the Corescan data on one hand and the global series resistance of the cell on the other hand are complex three dimen-

sional modeling problems that are beyond the scope of this paper.

In summary we have demonstrated an improved method to access local effective R_S -values by PL imaging. The method allows measuring the spatially resolved series resistance at different operating points by variation in the operating point in the first image. The main assumption in this method is that the light generated current density $J_{\text{light},i}$ is homogeneous across the cell area and equal to the short circuit current density. Assumptions and approximations in relation to $J_{\text{dark},i}(U_i)$ and the associated errors in previous R_S -imaging methods are avoided in this method. In addition, the requirement to access the local calibration constant C_i , needed to convert the local luminescence signal into an absolute local diode voltage, has been eliminated. Problems associated with the unknown dependency of C_i on the local carrier diffusion length and therefore on U_i are thereby also avoided.

The authors would like to thank Martin Kasemann from Fraunhofer ISE for providing the cell investigated in this study and Jessie Copper for performing Corescan measurements. H.K. would also like to thank the Centre of Excellence for Advanced Silicon Photovoltaics, UNSW, in particular Martin Green for financial support. The Centre of Excellence for Advanced Silicon Photovoltaics and Photonics is supported under the Australian Research Council's Centres of Excellence Scheme.

¹A. S. H. van der Heide, A. Schönecker, G. P. Wyers, and W. C. Sinke, Proceedings of the 16th European Photovoltaic Solar Energy Conference, 2000 (unpublished), p. 1438.

²J. Carstensen, G. Popkurov, J. Bahr, and H. Föll, *Sol. Energy Mater. Sol. Cells* **76**, 599 (2003).

³O. Breitenstein, J. P. Rakotoniaina, A. S. H. van der Heide, and J. Carstensen, *Prog. Photovoltaics* **13**, 645 (2005).

⁴J. Isenberg, A. S. H. van der Heide, and W. Warta, Proceedings of the 31st IEEE Photovoltaic Specialists Conference (unpublished), p. 907.

⁵T. Trupke, R. A. Bardos, M. D. Abbott, F. W. Chen, J. E. Cotter, and A. Lorenz, WCEC-4, Hawaii, 2006 (unpublished).

⁶T. Trupke, E. Pink, R. A. Bardos, and M. D. Abbott, *Appl. Phys. Lett.* **90**, 093506 (2007).

⁷K. Ramspeck, K. Bothe, D. Hinken, B. Fischer, J. Schmidt, and R. Brendel, *Appl. Phys. Lett.* **90**, 153502 (2007).

⁸D. Hinken, K. Ramspeck, K. Bothe B. Fischer, and R. Brendel, *Appl. Phys. Lett.* **91**, 182104 (2007).

⁹K. Schick, E. Daub, S. Finkbeiner, and P. Würfel, *Appl. Phys. A: Solids Surf.* **54**, 109 (1992).

¹⁰T. Trupke, R. A. Bardos, M. D. Abbott, and J. E. Cotter, *Appl. Phys. Lett.* **87**, 093503 (2005).

¹¹T. Fuyuki, H. Kondo, T. Yamazaki, Y. Takahashi, and Y. Uraoka, *Appl. Phys. Lett.* **86**, 262108 (2005).

¹²T. Fuyuki, H. Kondo, Y. Kaji, T. Yamazaki, Y. Takahashi, and Y. Uraoka, Proceedings of the 31st IEEE Photovoltaic Specialists Conference, 2005 (unpublished).